Organic & Biomolecular Chemistry

PAPER

View Article Online
View Journal | View Issue

Cite this: *Org. Biomol. Chem.*, 2015, **13**, 3280

Xanthenones: calixarenes-catalyzed syntheses, anticancer activity and QSAR studies†

Daniel Leite da Silva,[a] Bruna Silva Terra,[a] Mateus Ribeiro Lage,[b] Ana Lúcia Tasca Góis Ruiz,[c] Cameron Capeletti da Silva,[d] João Ernesto de Carvalho,[c] José Walkimar de Mesquita Carneiro,[b] Felipe Terra Martins,[d] Sergio Antonio Fernades[e] and Ângelo de Fátima*[a]

Received 16th December 2014,
Accepted 16th January 2015

DOI: 10.1039/c4ob02611j

www.rsc.org/obc

An efficient method is proposed for obtaining tetrahydrobenzo[*a*]xanthene-11-ones and tetrahydro-[1,3]-dioxolo[4,5-*b*]xanthen-9-ones. The method is based on the use of *p*-sulfonic acid calix[*n*]arenes as catalysts under solvent-free conditions. The antiproliferative activity of fifty-nine xanthenones against six human cancer cells was studied. The capacity of all compounds to inhibit cancer cell growth was dependent on the histological origin of the cells. QSAR studies indicate that among compounds derived from β-naphthol the most efficient compounds against glioma (U251) and renal (NCI-H460) cancer cells are those having higher hydrogen bonding donor ability.

Introduction

Cancer is an important public health concern and a leading cause of death. It accounted for eight million deaths worldwide (*ca.* 15% of all deaths) in 2010 (38% more than in 1990).[1,2] Many of the current chemotherapy drugs have low specificity for tumor cancer cells, and are also toxic to normal cells. The inefficiency of existing drugs against different types of cancer issues, as well as the increasing emergence of strains resistant to these drugs are also reported.[3] Indeed, one of the biggest challenges of combating cancer is the development of new anticancer agents that are safe and effective.

Xanthenones are important biologically active heterocyclic compounds, with remarkable biological and medicinal properties, such as antiviral,[4] anti-inflammatory,[5] antiproliferative[6] and antibacterial activities.[7] Furthermore these compounds are also used as dyes,[8] as probes for fluorescence-based detection of biomolecules[9] and in laser technologies.[10] Xanthenones are also investigated for agricultural use as bactericide agent[7] and as photosensitizers in photodynamic therapy.[11]

Multicomponent reaction (MCR) approaches, using a phenolic compound, aldehydes and 1,3-dicarbonyl compounds under acid-catalyst effect, are used for the synthesis of xanthones.[12–14] In recent years, use of calix[*n*]arenes as catalyst has received considerable interest in organic synthesis, particularly in MCRs.[15] Calix[*n*]arenes are macrocyclic compounds synthesized by the *ortho*-condensation of *para*-substituted phenols and formaldehyde under base conditions. There are a large number of applications involving calix[*n*]arenes due to their easy structural modification.[15–17] In the last two decades, the chemical literature has reported numerous applications of calix[*n*]arenes in supramolecular chemistry.[18] Among all calix[*n*]arenes known so far, *p*-sulfonic acid calix[*n*]arenes showed to be the most efficient catalysts for Biginelli,[19] Povarov,[20,21] Mannich-type[22] and esterification[23] reactions. Although calix[*n*]arenes as catalysts in various reactions has been reported, there is no report in the literature on the use of these compounds as catalysts in the synthesis of xanthenones.

The facile synthesis based on MCR approaches and the diverse biological profile exhibited by xanthenones brought new perspectives for the development of new drugs based on this class of compounds. Herein, we report on the synthesis of fifty-nine xanthenones, an investigation of their *in vitro* antiproliferative activity on six human cancer cell types and some structure–activity relationship (SAR) studies.

[a]*Grupo de Estudos em Química Orgânica e Biológica (GEQOB), Departamento de Química, Instituto de Ciências Exatas, Universidade Federal de Minas Gerais, Belo Horizonte, MG 31270-901, Brazil. E-mail: adefatima@qui.ufmg.br; Fax: +55-31-3409-5700; Tel: +55-31-3409-6373*
[b]*Instituto de Química, Universidade Federal Fluminense, Campus do Valonguinho, Niterói, RJ 24220-900, Brazil*
[c]*Centro Pluridisciplinar de Pesquisas Químicas, Biológicas e Agrícolas (CPQBA), Universidade Estadual de Campinas, Paulínia, SP 13081-970, Brazil*
[d]*Instituto de Química, Universidade Federal de Goiás, Goiânia, GO 74690-900, Brazil*
[e]*Grupo de Química Supramolecular e Biomimética (GQSB), Departamento de Química, Universidade Federal de Viçosa, Viçosa, MG 36570-900, Brazil*
† Electronic supplementary information (ESI) available. CCDC 1002985. For ESI and crystallographic data in CIF or other electronic format see DOI: 10.1039/c4ob02611j

Results and discussion

We report herein an easy-to-do and solvent-free three-component synthesis of xanthenones in the presence of a catalytic quantity of the calix[*n*]arenes **CX1**–**CX6** (Fig. 1). Xanthenones were synthesized using aldehydes, a 1,3-dicarbonyl compound, β-naphthol or sesamol as starting materials. First we focused on the screening of a series of calix[*n*]arenes (Fig. 1) as catalysts in reactions containing β-naphthol, 4-fluoro-benzaldehyde and dimedone at 120 °C under solvent-free conditions (Table 1). Among the calix[*n*]arenes tested in the range of 0.15–2.0 mol%, **CX3** and **CX6** were the most efficient catalysts. Both **CX3** and **CX6** at 1.5 mol% furnished the xanthenone **4** in 74% and 68% yields, respectively (Table 1; entries 5 and 10, respectively).

Amounts of **CX3** or **CX6** lower than 1.0 mol% (Table 1; entries 2 and 3 for **CX3**, and entries 7 and 8 for **CX6**) or higher than 1.5 mol% (Table 1; entries 6 and 11, for **CX3** and **CX6**, respectively) provided **4** in poor to moderate yields. The yield of reactions in the presence of 1.5 mol% calix[*n*]arenes **CX1**, **CX2**, **CX4** or **CX5** was comparable to that of catalyst-free reactions (Table 1; entry 1).

We also evaluated whether calix[*n*]arenes **CX3** or **CX6** could be reused in such reactions. After completing the reaction, $CHCl_3$ and water were added to the mixture in order to recover

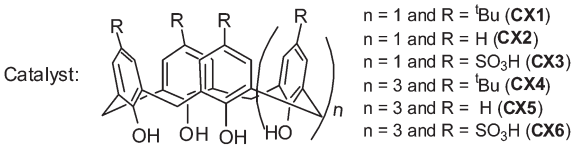

Fig. 1 Structure of calix[*n*]arenes evaluated as catalyst.

Table 1 Effect of the quantity of *p*-sulfonic acid calix[*n*]arenes of xanthenone **4** based on the amount of catalyst[a]

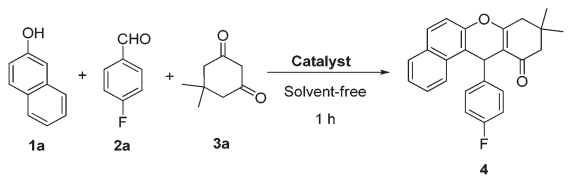

Entry	Catalyst (mol%)	Yield[b] (%)
1	—	16
2	**CX3** (0.15)	53
3	**CX3** (0.5)	57
4	**CX3** (1.0)	61
5	**CX3** (1.5)	74
6	**CX3** (2.0)	63
7	**CX6** (0.15)	54
8	**CX6** (0.5)	61
9	**CX6** (1.0)	64
10	**CX6** (1.5)	68
11	**CX6** (2.0)	67

[a] Reagents and conditions: β-naphthol/4-fluoro-benzaldehyde/dimedone (molar ratio of 1.2 : 1.0 : 1.5), 120 °C for 1 h. [b] Isolated yield.

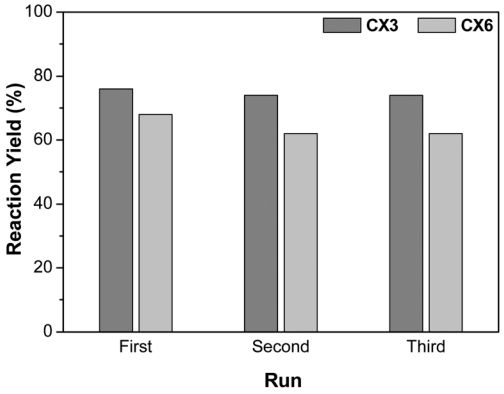

Fig. 2 Reuse of *p*-sulfonic acid calix[*n*]arenes **CX3** and **CX6** in the synthesis of xanthenone **4**.

CX3 or **CX6** in the aqueous phase from the reaction medium. Once dried, the residue was used in successive reactions in which the yields were monitored. **CX3** and **CX6** were successfully used in three successive reactions without significant loss of catalyst activity (Fig. 2).

Considering that yields of reactions in the presence of either **CX3** or **CX6** were roughly the same (Table 1, entries 5 and 10, respectively) we chose the former to evaluate the scope of *p*-sulfonic acid calix[4]arene for the synthesis of xanthenones. Thus, a variety of aldehydes, 1,3-dicarbonyls and two phenolic compounds were used (Table 2). Fifty-nine xanthenones (**4**–**62**) were synthesized with yields in the range 58–92%. The reaction yields were not considerably affected by the presence of electron-withdrawing or electron-donating groups in the aldehydes (Table 2).

Once synthesized, the structural characterizations of the xanthenones were determined from the corresponding IR, NMR (^{1}H and ^{13}C) and ESI-HRMS data. Crystals of **4** were also obtained and its crystal structure was determined using single-crystal X-ray diffractometry. Crystal data and refinement results are provided as ESI (Table S1†). Xanthenone **4** crystallizes in the triclinic system (space group *P*1). Both *R* and *S* enantiomers are present in the chosen crystallographic asymmetric unit (Fig. 3). Their molecular conformation is similar. Moreover, they cannot be related by centrosymmetry in the crystal lattice. Therefore, the crystal structure could not be solved in the centrosymmetric triclinic space group with only one molecule in the asymmetric unit. The xanthenone core, formed with the four fused rings labeled as A–D in Fig. 3, is approximately planar, except for ring A which assumes a half-chair conformation with C3 deviating away from the least-squares plane calculated through the other five coplanar atoms of this ring by −0.631(7) Å in the *R*-enantiomer (atom labels ending with suffix A) and 0.660(6) Å in the *S*-enantiomer (atom labels ending with suffix B) (r.m.s.d. of the C2–C1–C6–C5–C4 fitted atoms is 0.0292 Å in the *R*-enantiomer and 0.0205 Å in the *S*-enantiomer). Ring B is not completely planar in both enantiomers, with C7 carbon deviating by −0.270(6) Å in the *R*-enantiomer and 0.212(6) Å in the *S*-enantiomer from the least-square mean plane calculated through the

Table 2 Synthesis of xanthenones catalyzed by the *p*-sulfonic acid calix[4]arene **CX3**[a]

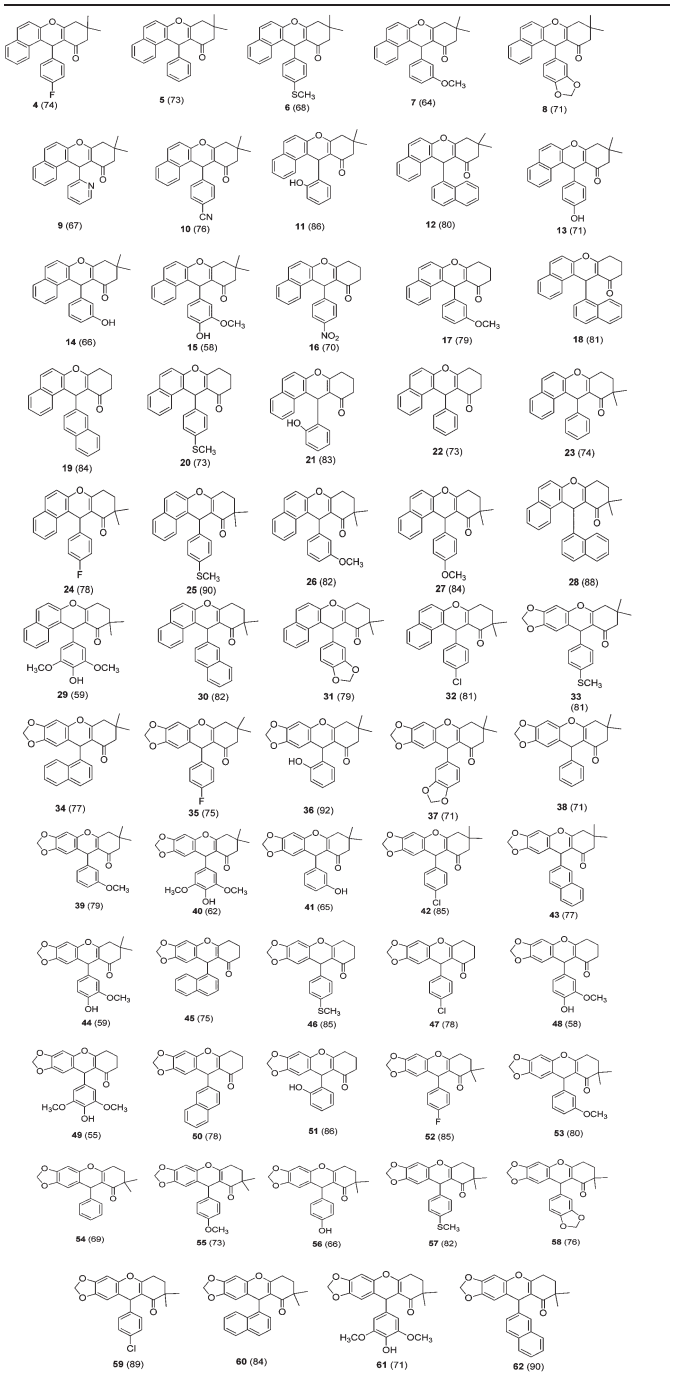

[a] Reagents and conditions: phenolic compound/aldehyde/1,3-dicarbonyl compound (molar ratio of 1.2 : 1.0 : 1.5), 120 °C for 1 h. The yield for obtaining each xanthenone is presented in parentheses.

C6–C5–O2–C9–C8 atoms (r.m.s.d. of the fitted atoms is 0.0431 Å in the *R*-enantiomer and 0.0270 Å in the *S*-enantiomer). Taking the xanthenone mean plane as reference, the out-of-plane C3 and C7 carbons are on the same side of the fluorinated phenyl ring in both enantiomers. Another intramolecular feature common to both enantiomers is the substituted

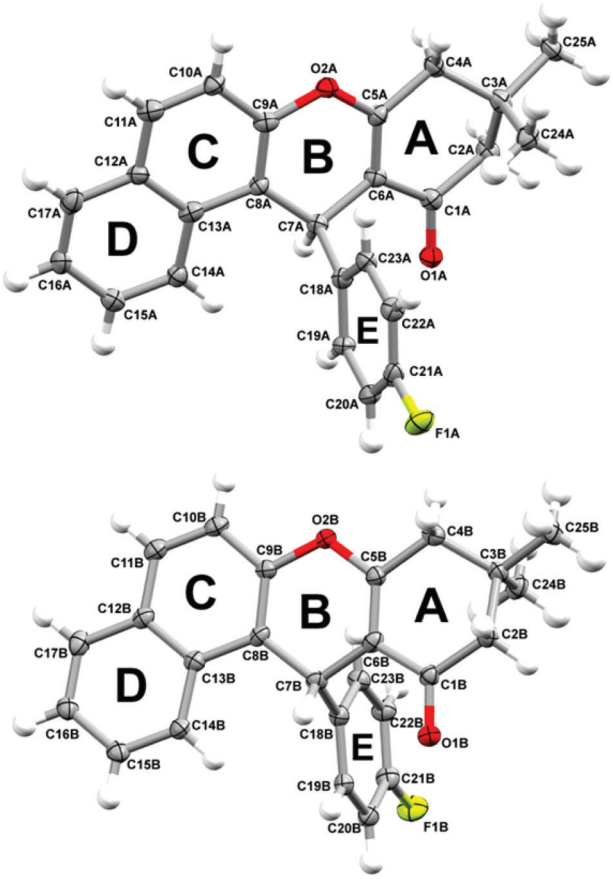

Fig. 3 The two crystallographically independent molecules of compound **4**. Ellipsoids of 30% probability and arbitrary radius spheres represent non-hydrogen and hydrogen atoms, respectively. Rings are also arbitrarily labeled.

phenyl ring conformation. Ring E is almost perpendicular to the xanthenone mean plane, forming an angle of 82.04(12)° in the *R*-enantiomer and 84.33(17)° in the *S*-enantiomer with the least-square plane calculated through the planar non-hydrogen atoms of the four fused rings A–D. Therefore, C3 and C7 were not included in this mean plane calculation.

Antiproliferative activity

Although xanthenones are known as bioactive heterocyclic compounds, only few works explored the potential of this class of compounds against cancer cells. Based on this, the antiproliferative effect of a series of synthesized xanthenones were investigated on glioma (U251), breast (MCF-7), multiple drugs-resistant ovarian (NCI-ADR/RES), renal (786-0), lung non-small cells (NCI-H460), colon (HT-29), and keratinocyte (HaCaT). Cell proliferation was determined by the sulforhodamine B method and doxorubicin (Dox) used as a positive control.[24]

Initially the fifty-nine xanthenones synthesized were subdivided into two groups of compounds according to the precursor phenol structure. Group 1 consisted of β-naphthol-derived xanthenones (**4–32**; Table 2) while **33–62** (Table 2), sesamol derivatives, were included in Group 2. The concentration of

the most active xanthenones that elicited 50% cell growth inhibition (GI_{50}) is summarized in Table 3. The GI_{50} values for the remainder of the compounds tested are provided as ESI (Table S2†).

When analyzing the data obtained for compounds of Group 1 (Table 3) it was noted that the NCI-ADR/RES cell line was the most sensitive cancer cells as attested by the number of compounds that negatively affected cells growth at $GI_{50} \leq 10$ μg mL^{-1} (Table 3). NCI-H460 cells were the least sensitive to compounds of Group 1 (Table 3).

For NCI-ADR/RES nineteen compounds of Group 1 showed GI_{50} values lower than 10 μg mL^{-1}. The active compounds of Group 1 for this strain showed GI_{50} values in the range of 0.027 to 9.8 μg mL^{-1}. Among the active compounds of Group 1 for NCI-ADR/RES cell line compound **5** was the most potent, with an GI_{50} value of 0.027 μg mL^{-1}, its GI_{50} value was found to be in the same order of magnitude of that for doxorubicin (GI_{50} = 0.047 μg mL^{-1}) (Table 3). Indeed, xanthenone **5** showed high selectivity index for NCI-ADR/RES cancer cells, presenting weak antiproliferative activity against non-tumorogenic HaCat cells (Table 3). Xanthenones **7**, **9**, **13**, **15**, **16**, **23** and **29** were also promising against NCI-ADR/RES cells by exhibiting GI_{50} around 1 μg mL^{-1} (Table 3). Xanthenones **13**, **15**, and **29** were the most potent compounds against NCI-H460 cells; its GI_{50} value were lower than 5.0 μg mL^{-1}. MCF7 cells were highly sensitive to xanthenones **8**, **9**, **13–15**, **24** and **29** (Table 3). Compounds **13–15**, **20** and **29** compromised U251 cell growth by 50% when used at concentrations lower than 6.5 μg mL^{-1}, while 786-0 cells were sensitive to **4**, **6**, **8**, and **29**. For HT-29 cells compounds **13–15**, and **29** were the most potent with GI_{50} values lower than 4.0 μg mL^{-1}. Among the tested compounds of Group 1, xanthenones **13**, **15**, **29** were those that exhibited the largest spectrum of action. These xanthenones showed considerable antiproliferative activity (GI_{50} < 10 μg mL^{-1}) against all the cancer cell lines, except for kidney cancer cell line (786-0) in which xanthenones **13** and **15** presented GI_{50} values of 216.0 and 29.8 μg mL^{-1}, respectively (Table 3).

The second group of xanthenones evaluated (Group 2) is related with those compounds derived from sesamol (Table 3, compounds **33–62**). The antiproliferative activity of these compounds was expressed as the concentration that produced 50% cell growth inhibition or a cytostatic effect (GI_{50}, μg mL^{-1}) for each cell line (Table 3). Data obtained for compounds of Group 2 (Table 3) shows that MCF7 was the most sensitive cancer cell line as attested by the number of compounds that negatively affected cell growth at $GI_{50} \leq 10$ μg mL^{-1}. Nine compounds were active against MCF7, and **48** was the most potent with GI_{50} of 0.7 μg mL^{-1}. Compounds **48** also compromised U251, NCI-ADR/RES, and HT-29 cells growth by 50% when used at concentrations lower than 1.0 μg mL^{-1} while NCI-ADR/RES cells were sensitive to other six compounds **36**, **39**, **41**, **43** and **45**, and **49**. For HT-29 cells compounds **41**, **45**, **49** and **56** were the most potent with GI_{50} values lower than 4.0 μg mL^{-1}. Kidney cell line (786-0) was the least sensitive strain to com-

Table 3 Selective index (SI)[a] and concentration of the most active xanthenones (GI_{50} [b] in μg mL^{-1}) that elicits cancer cells[c] growth inhibition by 50%

		U251		MCF7		NCI-ADR/RES		786–0		NCI-H460		HT-29		HaCaT
Group	Xanthenone	GI_{50}	**SI**	GI_{50}	**SI**	GI_{50}	**SI**	GI_{50}	**SI**	GI_{50}	**SI**	GI_{50}	**SI**	GI_{50}
1	**4**	186.6	0.2	203.7	0.2	2.0	16.1	3.1	10.3	36.3	0.9	>250	<0.1	32.1
1	**5**	56.8	0.8	92.0	0.5	0.03	1626	28.9	1.5	85.8	0.5	>250	<0.2	43.9
1	**6**	>250	<0.4	61.4	1.6	>250	<0.4	2.8	35.3	81.7	1.2	>250	0.4	98.9
1	**7**	29.8	1.8	56.9	1.0	0.8	70.3	>250	<0.2	50.5	1.1	>250	<0.2	54.1
1	**8**	28.5	0.9	2.0	12.9	227.9	0.1	1.7	15.1	28.7	0.9	48.2	0.5	25.7
1	**9**	25.6	0.9	5.2	4.5	0.7	33.3	27.1	0.9	31.4	0.7	29.9	0.8	23.3
1	**11**	14.0	3.8	>250	<0.2	67.5	0.8	225.4	0.2	>250	<0.2	>250	<0.2	52.9
1	**13**	2.9	2.1	2.6	2.3	0.4	15.2	216.0	0.03	2.8	2.2	3.2	1.9	6.1
1	**14**	2.9	2.0	2.7	2.1	6.7	0.9	>250	<0.02	13.1	0.4	3.2	1.8	5.8
1	**15**	2.9	6.9	3.9	5.2	0.3	67.0	29.8	0.7	2.6	7.7	3.4	5.9	20.1
1	**16**	94.0	2.7	100.3	2.5	0.4	625	197.4	1.3	119.9	2.1	>250	—	>250
1	**20**	6.5	4.4	21.5	1.3	8.9	3.2	20.4	1.4	19.6	1.4	16.0	1.8	28.4
1	**21**	84.5	2.4	127.0	1.6	51.9	3.9	246.3	0.8	>250	<0.8	>250	<0.8	204.6
1	**23**	35.1	1.0	82.4	0.4	0.1	341	188.3	0.2	60.3	0.6	95.9	0.4	34.1
1	**24**	25.1	0.6	8.8	1.8	4.4	3.5	76.6	0.2	44.2	0.3	16.2	1.0	15.4
1	**29**	2.9	2.4	2.8	2.5	0.4	17.8	4.9	1.4	4.3	1.7	2.9	2.4	7.1
2	**36**	25.2	1.1	24.4	1.1	9.3	2.9	26.2	1.0	24.3	1.1	19.4	1.4	26.6
2	**39**	37.2	0.3	5.7	2.3	7.2	1.8	110.3	0.1	27.8	0.5	4.9	2.6	12.9
2	**41**	3.4	1.2	3.0	1.3	4.9	0.8	4.0	1.0	5.0	0.8	3.5	1.1	4.0
2	**43**	29.5	1.1	26.3	1.2	8.6	3.8	28.5	1.1	26.1	1.2	25.1	1.3	32.6
2	**45**	5.3	0.8	3.2	1.3	5.4	0.8	25.0	0.1	10.5	0.4	2.6	1.7	4.3
2	**48**	0.7	1.1	0.7	1.1	0.5	1.6	2.2	0.4	2.3	0.3	0.43	1.9	0.80
2	**49**	3.3	0.8	2.2	1.3	1.6	1.8	7.1	0.4	7.3	0.4	2.7	1.0	2.8
2	**56**	3.3	1.1	2.9	1.2	12.9	0.3	>250	<0.01	3.1	1.1	2.7	1.3	3.5
—	**Dox**[d]	0.03	7.4	0.06	3.4	0.05	4.0	0.04	5.3	0.01	15.4	0.08	2.4	0.2

[a] Selectivity index was determined as the ratio of the GI_{50} for HaCat to the GI_{50} for the cancer cell line. [b] GI_{50} values were obtained from two independent experiments, each done in triplicate. [c] U251, glioma cells; MCF7, breast; NCI-ADR/RES, multiple drug-resistant ovarian cancer cells; 786-0, renal cancer cells; NCI-H460, non-small lung cancer cells; HT-29, colon cancer cells; HaCaT, keratinocyte. [d] Reference drug.

pounds of Group 2, as for this line only compounds **41**, **48** and **49** were active, with GI_{50} values of 4.0, 2.2 and 7.1 μg mL^{-1}, respectively. For NCI-H460 strain compounds **41**, **48**, **49** and **56** were active compounds of Group 2. Compounds **48** (GI_{50} = 2.3 μg mL^{-1}) and **56** (GI_{50} = 3.1 μg mL^{-1}) exhibited GI_{50} values lower than 4.0 μg mL^{-1}, thus showing potent anticancer activity. Among compounds of Group 2, **41**, **48** and **49** were those showing the highest spectrum of action, which were active against the six cancer cell lines evaluated. Compound **48** showed GI_{50} values lower than 4.0 μg mL^{-1} for all tested strains and can therefore be described as the most promising compound among compounds of Group 2.

The selectivity index (SI) was calculated for each compound of Group 1 and 2 (Table 3). Among evaluated xanthenones, compound **5** showed the highest SI value for NCI-ADR/RES cells, which indicated the potential use of this compound for future *in vivo* tests.

When comparing the results obtained for compounds of Group 1 and 2, we can see that in general compounds of Group 1 were more active than the compounds of Group 2. Among compounds of Group 1 evaluated eight compounds showed no activity against any of the tested strains, whereas eighteen compounds of Group 2 were inactive for all cell lines evaluated. Together these results suggest that the naphthyl nucleus is important for the antiproliferative activity of this class of compound. Overall, the potency of xanthenones was dependent on the histological origin of cancer cells.

QSAR studies

For a more careful analysis of the relationship between molecular structure and biological activity, QSAR studies were performed. To determine the correlation between molecular descriptors and the efficiency of the set of xanthenones, we tested a set of models as discussed below.

At first, a structural analysis of the studied compounds was carried out. The geometries of the 59 synthesized compounds were obtained from AM1 semiempirical calculations, after a conformational analysis using the conformer distribution subroutine of the SPARTAN'06 software. The most stable conformation of each derivative was then reoptimized with MOPAC software, again using the AM1 method. The output files from the MOPAC calculation were used to generate a set of molecular descriptors by using the CODESSA software.

CODESSA may generate about 400 molecular descriptors associated with molecular constitution, geometry, and topology and with electrostatic, thermodynamic, and quantum chemical parameters. The molecular descriptors generated by CODESSA were correlated to the biological efficiency using the heuristic method.[25] Models based on a single molecular descriptor were chosen to obtain statistically significant meanings. After elimination of descriptors with low variance or high intercorrelation, the best correlations were found with the molecular descriptors for compounds of Group 1 to cell lines U251 and NCI-H460. Compounds with GI_{50} > 250 μg mL^{-1} were not considered in the QSAR studies.

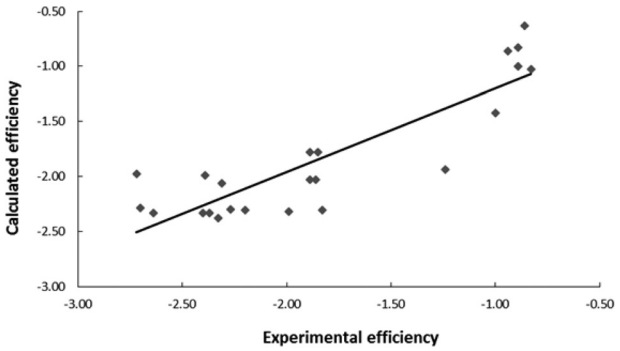

Fig. 4 Experimental *versus* calculated efficiency with the HDCA1 descriptor.

For U251 the best correlation was between experimental biological activity of compounds of Group 1 and the calculated efficiency based on the molecular descriptor HDCA-1.

HDCA-1 is a molecular descriptor that reports the hydrogen bonding donor ability of the molecule. The values of this descriptor are obtained as a sum of the accessible surface area of H-bonding donor H atoms, as described below.[26,27]

$$\mathrm{HDCA1} = \sum_{D} s_D \quad D \in H_{\text{H-donor}}$$

where s_D – solvent-accessible surface area of H-bonding donor H atoms.

The model obtained for U251 cells is given in Fig. 4 with the corresponding calculated efficiency *versus* measured efficiency plot.

This correlation indicates that increasing the accessible surface area of hydrogen bond donor atoms (HDCA1) leads to an increase in biological activity of the compound. This model shown to be consistent with the fact that compounds **13**, **14**, **15**, and **29**, which have a hydroxyl group in the *meta* or *para* position and have the highest values of HDCA1 molecular descriptor, were the most active against U251 cells. Although compounds **11** and **21** possess a hydroxyl group in the *ortho* position, this is less accessible than the *meta* or *para* positions resulting in lower values for the descriptor HDCA1 and experimental biological activity.

$$\mathrm{Log}\left(\frac{1}{\mathrm{IC}_{50}}\right) = 6.49 \times 10^{-1}(\pm 8.41 \times 10^{-2})(\mathrm{HDCA1}) - 2.46 \times 10(\pm 1.01 \times 10^{-1})$$
$$n = 23;\ r^2 = 0.764;\ F = 68.1;\ s^2 = 0.1067;\ {R_{\mathrm{cv}}}^2 = 0.731$$

The best correlation found for NCI-H460 cells was between the experimental biological activity of compounds of Group 1 and the calculated efficiency based on the molecular descriptor HDCA2. HDCA2 is a molecular descriptor based on accessible area of hydrogen-bond donor atoms and corresponds to partial charges.[26,27] The HDAC2 descriptor can be calculated as described below.

$$\mathrm{HDCA2} = \sum_{D} \frac{q_D \sqrt{s_D}}{\sqrt{S_{\mathrm{tot}}}} \quad D \in H_{\text{H-donor}}$$

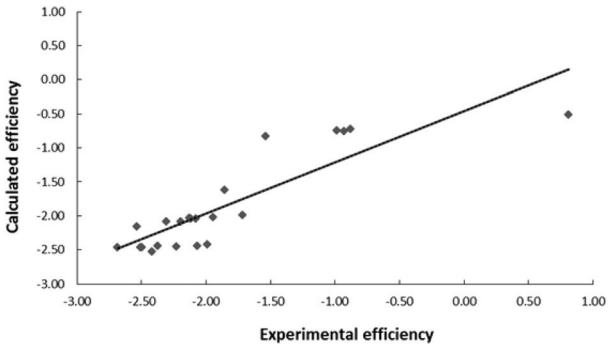

Fig. 5 Experimental *versus* calculated efficiency with the HDCA2 descriptor.

where s_D – solvent-accessible surface area of H-bonding donor H atoms; q_D – partial charge on H-bonding donor H atoms; S_{tot} – total solvent-accessible molecular surface area.

The model obtained for NCI-H460 cells is given in Fig. 5. This relation indicates that the activity values increase when increasing the value of the molecular descriptor HDCA2. This behavior is similar to that shown for U251 cells and the HDCA1 molecular descriptor. Again compounds **13**, **14**, **15**, and **29**, which have a hydroxyl group in the *meta* or *para* positions and have the highest values of HDCA2 molecular descriptor, were the most active against NCI-H460 cells and *ortho* hidroxilated compounds **11** and **21** were less active than *meta* or *para* hydroxylated derivatives. In summary, these two models shows that the activity of compounds of Group 1 against U251 and NCI-H460 increased with increase in accessible surface area of hydrogen bond donor atoms.

$$\mathrm{Log}\left(\frac{1}{\mathrm{IC}_{50}}\right) = 4.00 \times 10(\pm 5.06 \times 10^{-1})(\mathrm{HDCA2}) - 2.74 \times 10(\pm 1.39 \times 10^{-1})$$

$$n = 22;\ r^2 = 0.758;\ F = 62.5;\ s^2 = 0.159;\ {R_{cv}}^2 = 0.639$$

Conclusions

An efficient method was described for the synthesis of fifty nine xanthenones under mild conditions. The reaction yields dramatically increased upon the use of *p*-sulfonic acid calix[*n*]-arenes as catalysts. Some advantages of the approach here described include absence of solvents and metal catalysts, short reaction time, catalyst tolerance of a wide range of functional groups and catalyst recycling as well. The ability to inhibit the growth of cancer cells was also investigated for the synthesized compounds. Compound **5** was as potent as the reference drug doxorubicin against NCI-ADR/RES and present the greater value of SI. Several compounds were shown to be active against different cancer cell lines indicating that the capacity to inhibit cancer cell growth of the xanthenones was dependent on the histological origin of cells. In general, xanthenones derivatives of β-naphthol were more active than those derived from sesamol. A QSAR study was performed and two QSAR models were obtained for compounds of Group 1 against U251 and NCI-H460 cells and indicated that the biological activity of the compounds increased with increasing accessible surface area of hydrogen bond donor atoms. These results show some xanthenones as lead compounds for obtaining new anticancer agents.

Experimental

General methods and materials

All starting materials were obtained from commercially available sources with high-grade purity and used without further purification. Calix[*n*]arenes **CX1**–**CX6** were prepared according to known procedures.[28–30] Reactions did not require anhydrous conditions. The melting points (uncorrected) of synthesized xanthenones were determined on a Mettler FP 80 HT apparatus. Infrared spectra were recorded on a Perkin-Elmer Spectrum One spectrophotometer (KBr). The ^{1}H and ^{13}C-NMR spectra were recorded on a Bruker AVANCE DPX-200 spectrometry at 200 MHz to ^{1}H and 50 MHz to ^{13}C, in DMSO-d_6, $CDCl_3$ or pyridine-d_5. Coupling constants (J) are reported in Hertz (Hz). High resolution mass spectra (HRMS) were recorded on Shimadzu LC-IT-TOF Prominence system. Low temperature X-ray diffraction data were collected using an Enraf-Nonius Kappa-CCD diffractometer equipped with a CCD camera of 95 mm and κ-goniostat. No absorption correction was applied to the raw dataset due to the negligible absorption coefficient using graphite-monochromated Mo Kα beam (λ = 0.71073 Å). The structure was solved using the direct methods of phase retrieval and the model was refined by full-matrix least squares method based on F^2. Positions of hydrogens have followed a riding model with bond distances stereochemically constrained according to the bonded carbon. The isotropic thermal displacement parameters of hydrogens were either 20% (C–H hydrogens, except those in methyl moieties) or 50% (hydrogens in methyl moieties) greater than the equivalent isotropic parameter of the bonded carbon.

General procedure for the synthesis of xanthenones

A mixture of an aromatic aldehyde (1 mmol), 1,3-dicarbonyl compound (1.5 mmol) and β-naphthol or sesamol (1.2 mmol) and *p*-sulfonic acid calix[*n*]arene **CX3** or **CX6** (1.5 mol%) was stirred at 120 °C for 1 h. After completion of the reaction, methanol was added to the mixture and stirred for 30 min. Then the solid was filtered and washed with cold ethanol to afford the xanthenones **4–62** in high purity (Table 3). All xanthenones were characterized by ^{1}H, ^{13}C NMR, IR, HRMS (ESI) and melting point (see ESI† for reference).

Antiproliferative assay

Human tumor cell lines U251 (glioma), MCF-7 (breast) NCI-ADR/RES (multiple drugs-resistant ovarian), 786-0 (renal), NCI-H460 (lung, non-small cells), HT-29 (colon), and HaCaT (keratinocyte) were kindly provided by Frederick Cancer Research & Development Center-National Cancer Institute-

Frederick, MA, USA. Stock cultures were grown in RPMI 1640 (GIBCO BRL, Life Technologies) supplemented with 5% of fetal bovine serum and penicillin (final concentration of 1 mg mL^{-1}) and streptomycin (final concentration of 200 U mL^{-1}).[31,32] Cells in 96-well plates (100 μL cells per well) were exposed to xanthenones (0.25–250 μg mL^{-1}) for 48 h at 37 °C and 5% of CO_2. Afterward cells were fixed with 50% trichloroacetic acid, submitted to sulforhodamine B assay for cell proliferation quantitation at 540 nm.[24] The concentration of compound that inhibits cell growth by 50% (GI_{50}) was determined through non-linear regression analysis using software ORIGIN 7.5 (OriginLab Corporation). Doxorubicin was used as a reference drug. Results presented are from two independent experiments, each done in triplicate.

Computations

The conformational analysis of the 59 xanthenones was done using the conformer distribution subroutine of the SPARTAN'06 software.[33] The most stable conformation of each derivative was selected for further calculations with the MOPAC code,[34] again using the AM1[35] semiempirical method. In this new step the geometry optimization was developed with the MOPAC code and all structures were confirmed as a local minimum by calculation of the Hessian matrix force constant (no negative eigenvector).[36] Two sets of output files were obtained with the MOPAC code. In the first one the following keywords were used: AM1, PRECISE, XYZ, EF, ENPART, VECTORS, BONDS, PI, and POLAR. In the second one, which was used to calculate the thermodynamic properties, the following keywords were used: AM1, PRECISE, THERMO, ROT = 1, and XYZ. These output files from MOPAC calculations were used to the development of the initial CODESSA calculations, to generate a set of molecular descriptors used in the QSAR analysis, also developed by using the CODESSA software.[37] In the statistical analysis for the QSAR study the following parameters were employed: maximum number of descriptors per model, 1; criterion of significance of parameter, 0.01; level of high correlation, 0.99; level of intercorrelation significance, 0.8.

Acknowledgements

We acknowledge the following Brazilian agencies: Conselho Nacional de Desenvolvimento Cientifíco e Tecnológico (CNPq) for research fellowships (A.D.F., J.W.M.C., S.A.F.) and financial support; Fundção de Amparo à Pesquisa de Minas Gerais (FAPEMIG), Coordenação de Aperfeiçoamento de Pessoal de Nível Superior (Capes), and Fundação de Amparo à Pesquisa do Estado do Rio de Janeiro (FAPERJ). Authors are also thankful to Dr C.M. da Silva and L.S. Neto for critical reading of the manuscript.

References

1 R. Lozano, M. Naghavi, K. Foreman, *et al.*, *Lancet*, 2013, **380**, 2095–2128.
2 O. Nakash, I. Levav, S. Aguilar-Gaxiola, *et al.*, *Psychooncology*, 2014, **23**, 40–51.
3 B. A. Chabner and J. T. G. Roberts, *Nat. Rev. Cancer*, 2005, **5**, 65–72.
4 R. W. Lambert, J. A. Martin, J. H. Merrett, K. E. B. Parkes and G. J. Thomas, *CT Int. Appl*, WO9706178, 1997.
5 J. P. Poupelin, G. Saint-Rut, O. Fussard-Blanpin, G. Narcisse, G. Uchida-Ernouf and R. Lakroix, *Eur. J. Med. Chem.*, 1978, **13**, 67–71.
6 A. Kumar, S. Sharma, R. A. Maurya and J. Sarkar, *J. Comb. Chem.*, 2010, **12**, 20–24.
7 T. Hideo and J. Teruomi, *Jpn. Patent*, 56.005.480, 1981.
8 A. Banerjee and A. K. Mukherjee, *Biotech. Histochem.*, 1981, **56**, 83–85.
9 C. G. Knight and T. Stephens, *Biochem. J.*, 1989, **258**, 683–689.
10 O. Sirkencioglu, N. Talinli and A. J. Akar, *Chem. Res.*, 1995, **12**, 502.
11 R. M. Ion, A. Planner, K. Wiktorowicz and D. Frackowiak, *Acta Biochim. Pol.*, 1998, **45**, 833–845.
12 M. M. Heravi, H. Alinejhad, K. Bakhtiari, M. Saeedi, H. A. Oskooie and F. F. Bamoharram, *Bull. Chem. Soc. Ethiop.*, 2011, **25**, 399–406.
13 J. M. Khurana and D. P. Magoo, *Tetrahedron Lett.*, 2009, **50**, 4777–4780.
14 Z.-H. Zhang, H.-J. Wang, X.-Q. Ren and Y.-Y. Zhang, *Monatsh. Chem.*, 2009, **140**, 1481–1483.
15 J. B. Simões, D. L. da Silva, A. de Fátima and S. A. Fernandes, *Curr. Org. Chem.*, 2012, **16**, 949–971.
16 A. de Fátima, S. A. Fernandes and A. A. Sabino, *Curr. Drug Discovery Technol.*, 2009, **6**, 151–170.
17 E. V. V. Varejão, A. de Fátima and S. A. Fernandes, *Curr. Pharm. Des.*, 2013, **19**, 6507–6521.
18 P. Jose and S. Menon, *Bioinorg. Chem. Appl.*, 2007, **28**, 1–16.
19 D. L. da Silva, S. A. Fernandes, A. A. Sabino and A. de Fátima, *Tetrahedron Lett.*, 2011, **52**, 6328–6330.
20 J. B. Simões, A. de Fátima, A. A. Sabino, F. J. T. Aquino, D. L. da Silva, L. C. A. Barbosa and S. A. Fernandes, *Org. Biomol. Chem.*, 2013, **11**, 5069–5073.
21 J. B. Simões, A. de Fátima, A. A. Sabino, L. C. A. Barbosa and S. A. Fernandes, *RSC Adv.*, 2014, **4**, 18612–18615.
22 S. Shimizu, N. Shimada and Y. Sasaki, *Green Chem.*, 2006, **8**, 608–614.
23 S. A. Fernandes, R. Natalino, P. A. R. Gazolla, M. J. da Silva and G. N. Jham, *Tetrahedron Lett.*, 2012, **53**, 1630–1633.
24 A. Monks, D. Scudeiro, P. Skehan, R. Shoemaker, K. Paull, D. Vistica, C. Hose, J. Langley, P. Cronise, A. Vaigro-Wolff, M. Gray-Goodrich, H. Campbelli, J. Mayo and M. J. Boyd, *J. Natl. Cancer Inst.*, 1991, **83**, 757–766.
25 B. Xia, W. Ma, B. Zheng, X. Zhang and B. Fan, *Eur. J. Med. Chem.*, 2008, **43**, 1489–1498.
26 D. T. Stanton and P. C. Jurs, *Anal. Chem.*, 1990, **62**, 2323.
27 D. T. Stanton, L. M. Egolf, P. C. Jurs and M. G. Hicks, *J. Chem. Inf. Comput. Sci.*, 1992, **32**, 306.

28 C. D. Gutsche, B. Dhawan, K. H. No and R. Muthukrishnan, *J. Am. Chem. Soc.*, 1981, **103**, 3782–3792.
29 A. Casnati, N. D. Ca, F. Sansone, F. Ugozzoli and R. Ungaro, *Tetrahedron*, 2004, **60**, 7869–7876.
30 S. Shinkai, K. Araki, T. Tsubaki, T. Some and O. Manabe, *J. Chem. Soc., Perkin Trans. 1*, 1987, 2297–2299.
31 D. L. da Silva, F. S. Reis, D. R. Muniz, A. L. T. G. Ruiz, J. E. de Carvalho, A. A. Sabino, L. V. Modolo and A. de Fátima, *Bioorg. Med.Chem.*, 2012, **20**, 2645–2650.
32 S. R. Pacheco, T. C. Braga, D. L. da Silva, L. P. Horta, F. S. Reis, A. L. T. G. Ruiz, J. E. de Carvalho, L. V. Modolo and A. de Fátima, *Med. Chem.*, 2013, **9**, 889–896.
33 *Spartan'06*, Wavefunction, Inc., Irvine, CA.
34 J. J. P. Stewart, *MOPAC 2007, version 7*, 290 W Stewart Computational Chemistry, Colorado Springs, CO, 2007.
35 M. J. S. Dewar, E. G. Zoebisch and E. F. Healy, *J. Am. Chem. Soc.*, 1985, **107**, 3902–3909.
36 F. Jensen, *Introduction to computational chemistry*, John Wiley & Son Ltd, 2nd edn, 2007.
37 A. R. Katritsky, V. S. Lobanov and M. Karelson, *CODESSA: Reference Manual; Version 2*, University of Florida, 1996.